

# Efficient Epoxidation of Alkenes with Hydrogen Peroxide and Electrochemical Behavior in Water Over Heteropolymolybdate/Silica Nanocomposite

Hossein Salavati\*, Abbas Teimouri

Department of Chemistry, Payame Noor University (PNU), 19395-3697, Tehran, I.R. IRAN

\*E-mail: [hosseinsalavati@pnu.ac.ir](mailto:hosseinsalavati@pnu.ac.ir)

Received: 14 February 2017 / Accepted: 25 May 2017 / Published: 12 July 2017

---

A (PVMo/SiO<sub>2</sub>) nanocomposite catalyst was synthesized by immobilization of vanadium substituted heteropolymolybdate (PVMo) in mesoporous silica. The nanocomposite catalyst was characterized by different physico-chemical techniques such as elemental analysis, FT-IR, UV-Vis, XRD, SEM, TEM, BET and cyclic voltammetry. The PVMo/SiO<sub>2</sub> nanocomposite catalyst was used for alkene epoxidation with H<sub>2</sub>O<sub>2</sub> as oxidant, under agitation with magnetic stirring and ultrasonic irradiation. Effect of reaction parameters such as amount of oxidant and catalyst, reaction temperature and intensity of ultrasonic irradiation were studied. This catalyst can be recovered several times with little failure of its activity. The obtained consequences explained that the catalytic activity of the nanocomposite (PVMo/SiO<sub>2</sub>) was upper than that of chaste heteropolymolybdate..

---

**Keywords:** Heteropolyanion, nanocomposite, epoxidation, Ultrasonic irradiation.

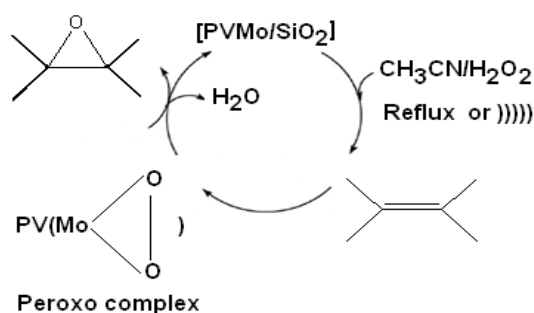
## 1. INTRODUCTION

Heteropolyacids (HPAs) demonstrate a wide collection of molecular sizes, compositions and architectures and have involved much attention as catalysts, because of their strong acidity and redox property, which can be restricted by replacing the protons with metal cations and / or by changing the heteroatom or the skeleton transition metal atoms [1-3]. The kegin type HPAs have been recognized as good catalysts for oxidation reactions [4, 5]. In recent years, there has been an growing interest in using transition metal-substituted polyoxometalates (TMSPs) as catalyst for the oxidation of organic substrates, in which the substituted vanadium is identified as the most active metal species [6,7]. Acid-base and oxidation reactions, catalyzed by solid heteropoly composites, can progress via three major techniques of reactions: surface, bulk type I (pseudo liquid) and bulk type II catalysis [8, 9].

In surface type catalysis, the reactions occur on the inner pore and outer surfaces of solid catalysts. In general, the reaction speed is comparative to the catalyst surface area. A valuable process for improving catalytic show in liquid-solid and gas-solid shell heterogeneous reactions is to maintain the heteropoly compounds on solids with lofty surface area. Other benefits of using supported heteropoly compounds as catalysts are their acceptance of improvement and recycling after operation liquid phase reactions, and the easier separation of produce than that of the homogeneously catalyzed reactions. Fundamental solids such as  $\text{Al}_2\text{O}_3$  and  $\text{MgO}$  as support have a tendency to decay the heteropoly compounds [10-12]. Acidic or neutral substances such as  $\text{SiO}_2$  [13-19], active carbon [20],  $\text{TiO}_2$  [21],  $\text{ZrO}_2$  [22], Polyaniline [23] are appropriate supports. Mesoporous silica has been established to be able to trap heteropoly acids, obtained elevated catalytic activity [24, 25]. Keggin-type transition metal substituted heteropolyoxoanions have some valuable properties that create them very good-looking as redox catalysts for roundabout electrochemical processes, such as

1. Elevated constancy in acidic media and inertness in the direction of reactive intermediates
2. Option to modify the official potential of the transition metal which is included into the polymetalate construction by altering the nature of the middle heteroatom;
3. Presence of extremely oxidized metallic centers, stabilized by the negatively charged polyoxo ligand, and extremely helpful in oxidation processes;
4. Incidence of an inner sphere electron transfer mechanism during the free co-ordination orbital of the transition metal [26].

In this research we expand our current study [18, 27-30]. Herein, we explain the synthesis and characterization of a new nanocomposite, consisting of vanadium substituted heteropolymolybdate  $\text{Na}_5\text{PV}_2\text{Mo}_{10}\text{O}_{40}$  (PVMo), supported on mesoporous silica. Under reflux and ultrasonic irradiation situations, supported and non-supported PVMo have been employed as catalysts for alkene epoxidation with hydrogen peroxide (Scheme 1).



**Scheme 1.** Oxidation of alkenes using  $\text{PVMo}/\text{SiO}_2$  catalyst

## 2. EXPERIMENTAL

### 2.1. Materials and methods

All chemicals were of reagent grade and used without extra purification. Vanadium substituted heteropolymolybdate (PVMo) was prepared according to the reported methods [31]. The mesoporous

silica used for support was Cab-oSil<sup>®</sup> M5 and prepared from Riedel-deHaen (Mesh 44 microns and Average particle length 0.2-0.3 microns). All other solvents and chemicals were bought from Merck Company and were obtained Cyclooctene, Cyclohexene, Indene,  $\alpha$ -Methylstyrene, Acetophenone,  $\alpha$ -Pinene, 1-dodecene, 1-octene.

Elemental analysis was performed on Perkin-Elmer NexIon 350 ICP-MS spectrometers. (Atomic Absorption analysis was carried out on a Shimadzu 120 spectrophotometer. Diffuse reflectance spectra (DRS) were recorded on a Shimadzu UV-265 apparatus with optical grade BaSO<sub>4</sub> as reference. Fourier-transformed infrared (FT-IR) spectra were obtained as potassium bromide pellets in the range of 400-4000 cm<sup>-1</sup> with Nicolet-Impact 400D apparatus. Scanning electron micrographs (SEM) of the catalyst and support were taken on SEM Philips XL 30. Powder X-ray diffraction (XRD) information were obtained on a D<sub>8</sub> Advanced Bruker, using Cu K $\alpha$  radiation ( $2\theta=5-70^\circ$ ). Gas chromatography (GC) experiments were performed with a Shimadzu GC-16A apparatus, using a 2 m column packed with silicone DC-200 or 20 m Carbowax. In all experiments the N-decane was used as internal standard. <sup>1</sup>H NMR spectra were recorded on a Bruker-Arance AQS 300 MHz. CDCl<sub>3</sub> and tetramethylsilane (TMS) were used as a solvent and an interior reference. Conversions and yields were obtained by GC experiments and the products were recognized after separation and purification. Cyclic voltammetric (CV) studies were performed with an Auto Lab 30 instrument.

## 2.2. Preparation of the PVMo/SiO<sub>2</sub> nanocomposite

To a solution of 0.1 g vanadium substituted heteropolymolybdate (PVMo) dissolved in 10 mL distilled water, was added 0.4 g pure mesoporous silica. The mixture was gently stirred under ambient circumstances for 20 h. The nanocomposite PVMo/ SiO<sub>2</sub> was isolated by evaporation of water and was dried at 60 °C under vacuum.

## 2.3. General procedure for epoxidation of alkenes with H<sub>2</sub>O<sub>2</sub> catalyzed by PVMo/ SiO<sub>2</sub> nanocomposite under reflux conditions

In a 25 mL round bottom flask prepared with a magnetic bar, was added 5 mL CH<sub>3</sub>CN, 1 mmol alkene, 1 mL of H<sub>2</sub>O<sub>2</sub> 30 % and 0.0475 mmol of PVMo/ SiO<sub>2</sub> catalyst and then refluxed. The reaction development was monitored by GC. At the end of reaction, the reaction mixture was diluted with CH<sub>2</sub>Cl<sub>2</sub> (10 mL), then filtered and the catalyst was thoroughly washed with CH<sub>2</sub>Cl<sub>2</sub>. The organic layer was purified on a silica-gel plate or a silica-gel column. IR and <sup>1</sup>H NMR spectral data established the identity of the products.

## 2.4. General procedure for epoxidation of alkenes with H<sub>2</sub>O<sub>2</sub> catalyzed by PVMo/ SiO<sub>2</sub> nanocomposite under ultrasonic irradiation

All reactions were carried out at room temperature in a 40 mL glass reactor. A UP 400S ultrasonic processor ready with a 3 mm wide and 140 mm long probe, which was wrapped up directly

into the reaction mixture, was used for sonication (irradiation power was  $100 \text{ w/cm}^2$ ). To a solution of alkene (1 mmol) in  $\text{CH}_3\text{CN}$  (10 mL), were added  $\text{H}_2\text{O}_2$  30% (1 mmol) and  $\text{PVMo/SiO}_2$  (0.0475 mmol) and showed to ultrasonic irradiation. The reaction development was monitored by GC. At the end of reaction, the reaction mixture was diluted with  $\text{CH}_2\text{Cl}_2$  (10 mL), then filtered and the catalyst was thoroughly washed with  $\text{CH}_2\text{Cl}_2$ . The organic layer was purified on a silica-gel plate or a silica-gel column. IR and  $^1\text{H}$  NMR spectral data established the identity of the products.

### 3. RESULTS AND DISCUSSION

#### 3.1. Characterization of the $\text{PVMo/SiO}_2$ nanocomposite

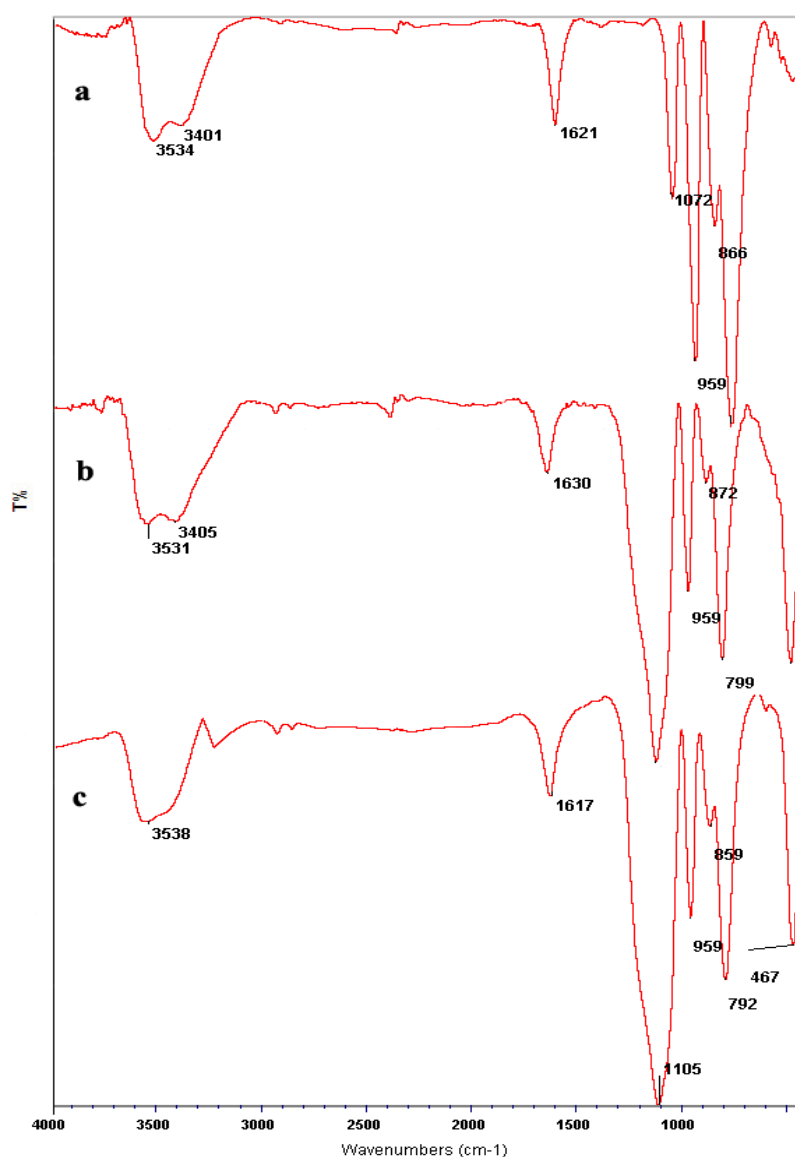


**Figure 1.** FT-IR spectra of: (a) PVMo; (b) nanocomposite  $\text{PVMo/SiO}_2$ ; and (c) recovered  $\text{PVMo/SiO}_2$

The presence of heteropolyanion supported on the silica, was confirmed by FT-IR spectra. In the FT-IR spectrum of PVMo, the bands in 1072, 959, 866, 787  $\text{cm}^{-1}$  could be credited to  $\nu(\text{P-O})$ ,  $\nu(\text{Mo-O})$ ,  $\nu(\text{Mo-O}_b\text{-Mo})$ ,  $\nu(\text{Mo-O}_c\text{-Mo})$  ( $\text{O}_b$ : corner-sharing oxygen,  $\text{O}_c$ : edge-sharing oxygen), respectively (Fig.1). The asymmetric stretching frequency of the terminal oxygens is observed at 959  $\text{cm}^{-1}$  and the P-O symmetric stretching frequency was appeared at 1072  $\text{cm}^{-1}$  [32]. Since FT-IR spectrum of the silica revealed a peak at 1100  $\text{cm}^{-1}$ , the PVMo band at 1072  $\text{cm}^{-1}$  zone was covered by the support band in the spectrum of the PVMo/  $\text{SiO}_2$ . These points approved that PVMo is successfully immobilized on the  $\text{SiO}_2$ . The UV-Vis absorption spectrum of PVMo in acetonitrile, displayed two absorption bands at 266 and 308 nm, which are associated with octahedral coordinated  $\text{Mo}^{6+}$  and ligand to metal charge transfer in the heteropoly cage [33, 34].

The diffuse reflectance spectrum of the PVMo/  $\text{SiO}_2$  nanocomposite resembles the solution counterpart spectrum with only a minor shift, which evidently showed the existence of PVMo on the silica (Fig. 2). Comparative of UV-Vis spectra of solution, before impregnation and after filtration of catalyst, indicated that more than 90% of PVMo supported on the silica.

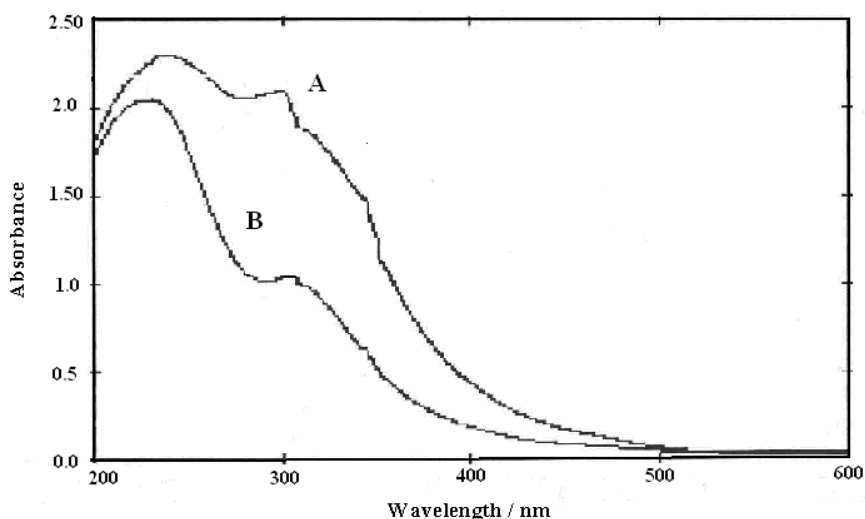


Figure 2. UV-Vis spectra of: (A) PVMo; (B) PVMo/  $\text{SiO}_2$

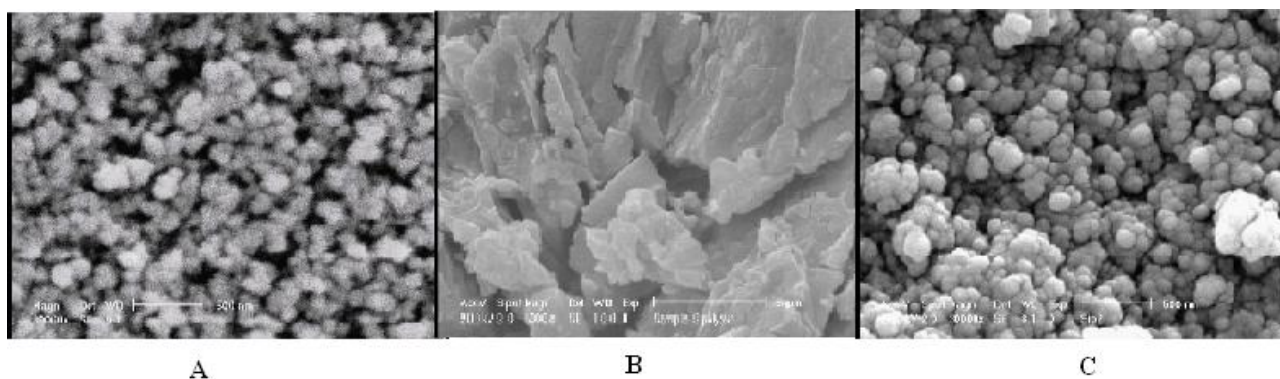
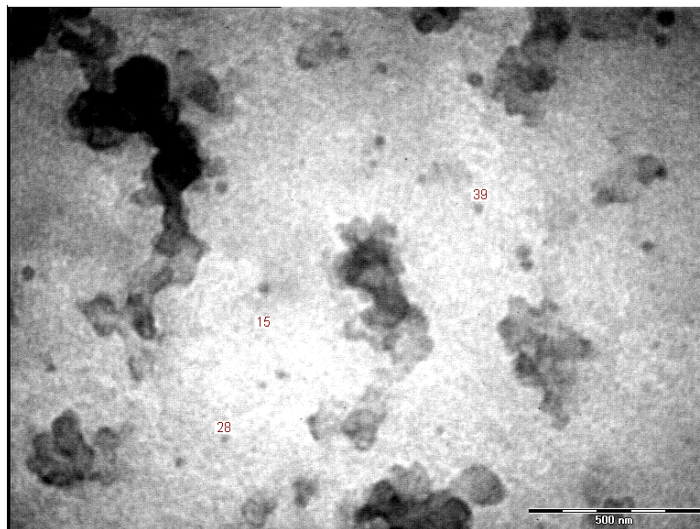
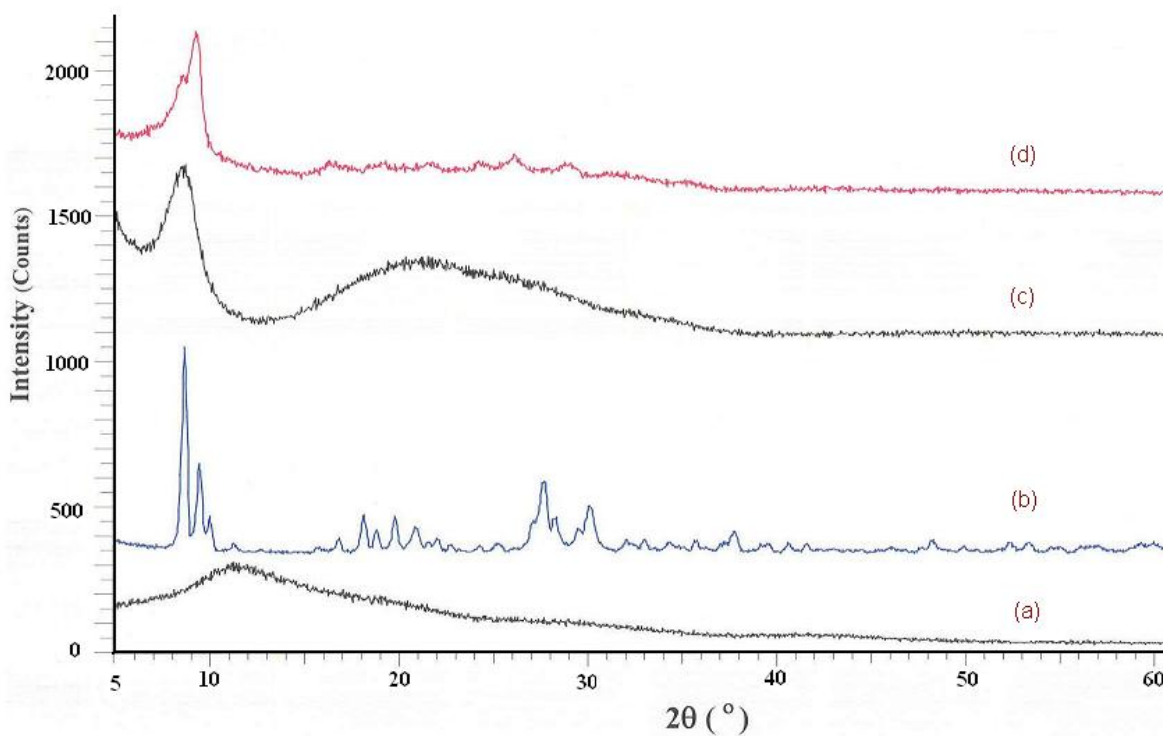


Figure 3. SEM of: (a)  $\text{SiO}_2$  nanoparticles; (b) PVMo; and (c) PVMo/  $\text{SiO}_2$

Scanning electron micrograph was recorded to attain the shape and diameter of particles (Fig. 3). The results indicated that spherical particles were fine dispersed and the average particle size was fewer than 40 nm. Transmittance Electron Microscopy (TEM) analysis was used to find out the position and size of the PVMo types which can be discriminated as dark dots in TEM (Fig. 4). The particle size obtained by this technique, was also less than 40 nm.



**Figure 4.** Transmission electron microscopy image of PVMo/ SiO<sub>2</sub>



**Figure 5.** XRD pattern of: mesoporous (a) SiO<sub>2</sub>; (b) PVMo; (c) PVMo/ SiO<sub>2</sub> (20%); and (d) PVMo/ SiO<sub>2</sub> (40%)

The Keggin category of the heteropolyanion was also proved by X-ray diffraction, which demonstrated typical peaks at  $2\theta$ :  $8.8^\circ$ ,  $9.2^\circ$ ,  $10.3^\circ$ ,  $27.9^\circ$  and  $29.2^\circ$  [31]. Obviously, the obtained sample belonged to the set of Keggin-type heteropolyanions (Fig. 5). The XRD patterns of  $\text{SiO}_2$  bulk, PVMO bulk and  $\text{SiO}_2$  containing 20 and 40 wt% of PVMO, are obtained in Fig. 5. No diffraction characteristic peaks for PVMO appeared in the spectra of catalyst containing 20% polyoxoanion. This is an effect of finely discreted PVMO in the porous structure of silica, and the composite behaves as X-ray amorphous. The XRD model for material with 40% of PVMO illustrates all the characteristic peaks of the polyoxoanion, therefore demonstrating that part of the PVMO is extra, and structures large enough crystallites in the superior pores of silica and on its external surface to provide a diffraction pattern.

In Fig. 6, nitrogen sorption isotherm of PVMO/ $\text{SiO}_2$  has been exposed. All samples were mesoporous, with  $\text{N}_2$  adsorption–desorption isotherms of kind IV according to the IUPAC categorization [35, 36]. The BET surface area of the material is  $210 \text{ m}^2 \text{ g}^{-1}$ . The values of  $P/P_0$  close to the inflection point are intimately connected to the pore-widths, which recline in the mesoporous range [37]. Pore size diameter of the sample anticipated employing the *Barrett-Joyner-Halenda* (BJH) technique is ca. 6.1 nm, which is in excellent accord with the pore widths predicted from the TEM image.

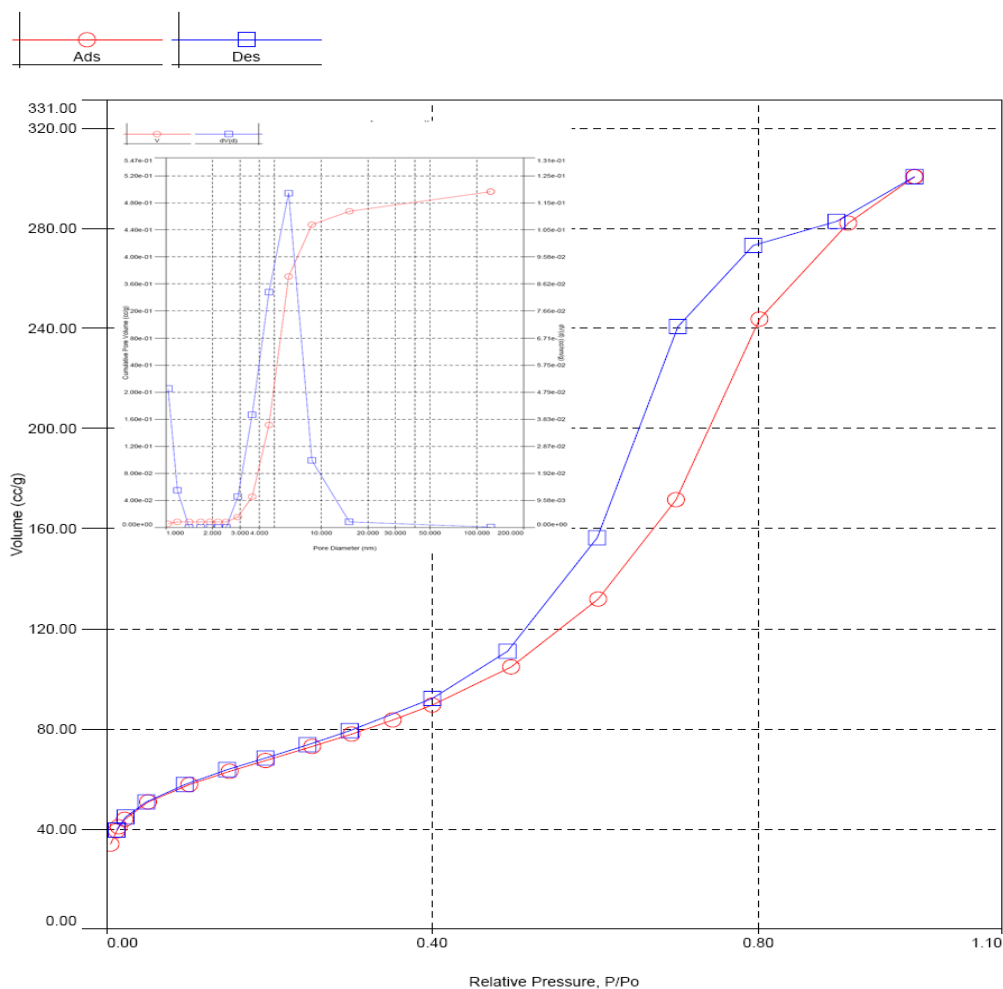


**Figure 6.**  $\text{N}_2$  adsorption–desorption isotherm of the PVMO/ $\text{SiO}_2$ . Inset: Pore size distribution using BJH method.

In addition, the BET surface areas and pore diameter of the samples are also offered in Table 1. In evaluation with the porous silica, both the BET surface area and pore volume of the PVMo/ SiO<sub>2</sub> catalyst have been shortened due to the preface of PVMo on the silica. The above experimental results illustrated that PVMo have been supported on the surface of silica based on electrostatic communication and keeping its electrochemical properties.

**Table 1.** The Special surface area, pore size and pore volume.

Sample	Specific surface Area (m <sup>2</sup> /g)	Pore size (nm)	Total pore volume (cm <sup>3</sup> /g)
SiO <sub>2</sub>	179.86	83.4	0.367
PVMo/SiO <sub>2</sub>	210	64.7	0.901

The electrochemistry of the [PMo<sub>(12-n)</sub>V<sub>n</sub>O<sub>40</sub>]<sup>(3+n)-</sup> species have been considered formerly [37, 38]. The aim of this part is to evaluate the electrochemistry of the PMo<sub>10</sub>V<sub>2</sub>O<sub>40</sub><sup>5-</sup> (PVMo) and SiO<sub>2</sub>-PMo<sub>10</sub>V<sub>2</sub>O<sub>40</sub><sup>5-</sup> (PVMo/ SiO<sub>2</sub>). The PVMo/ SiO<sub>2</sub> are not soluble in any solvent. Therefore, the electrochemical studies of PVMo and PVMo/ SiO<sub>2</sub> were approved in aqueous solution using carbon paste electrodes (CPEs) which were modified with PVMo and PVMo/ SiO<sub>2</sub>.

The mixture of 0.5 g PVMo/ SiO<sub>2</sub>, and 0.5 g graphite powder were mixed collectively. Then diethyl ether was added and mixture was mixed to obtain homogeneous mixture. After evaporation of diethyl ether, 0.3 g paraffin oil was added and the mixture was mixed with mortar and pestle to obtain a consistently wetted paste. The prepared paste was inserted in to a glass tube (internal radius 2.2 mm). To get ready a blank solution, 10.0 ml of the buffer solution (phosphate buffer, 0.10 M, pH 7.0) was transferred into an electrochemical cell. The differential pulse voltammogram (DPV) was recorded with a pulse height of 50 mV and a pulse width of 5 mV and the potential scanned from +0.20 and +0.70 V vs. Ag/AgCl.

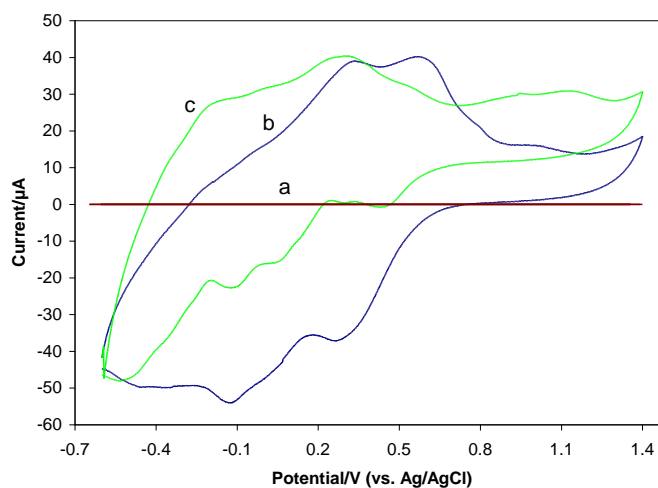


**Figure 7.** Cyclic voltammogram of: (a) bare CPE; (b) PVMo-CPE; and (c) PVMo/ SiO<sub>2</sub> -CPE in 0.2M H<sub>2</sub>SO<sub>4</sub> solution. Scan rate: 100mV s<sup>-1</sup>.

Figure 7, confirms the cyclic voltammograms in 0.2 M H<sub>2</sub>SO<sub>4</sub> aqueous solution at a naked CPE (Fig. 7a), PVMo-CPE (Fig. 7b) and a PVMo/ SiO<sub>2</sub>-CPE (Fig. 7c). It could be seen in Fig. 7 that in the potential variety of -0.6 to 1.4 V (vs. Ag/ AgCl), there is no redox peak at the naked CPE, while the voltammograms of PVMo-CPE and PVMo/ SiO<sub>2</sub>-CPE display some consecutive redox processes. Comparing the voltammograms of PVMo and PVMo/ SiO<sub>2</sub> illustrated that the immobilization of negatively charged PVMo on the surface of silica, led to a negative shift of the peak potentials and a raise in the separation of the peak potentials, which are in concord with the previously reported consequences [36]. This happening can be attributed to the interaction between the negatively charged redox couple and the oppositely charged silica matrix.

### 3.2. Alkene epoxidation with H<sub>2</sub>O<sub>2</sub> catalyzed by nanocomposite PVMo/ SiO<sub>2</sub> under reflux and ultrasonic irradiation conditions

At first, the nanocomposite PVMo/ SiO<sub>2</sub> with various catalyst loadings (PVMo) were arranged and considered their catalytic activity in the epoxidation of cyclooctene as model reaction with H<sub>2</sub>O<sub>2</sub>. The results proved that the nanocomposite catalyst with 20% loading of PVMo is more efficient (Table 2).

**Table 2.** Epoxidation of cyclooctene with H<sub>2</sub>O<sub>2</sub> (30%) catalyzed by PVMo/ SiO<sub>2</sub> with the diverse catalyst loading.<sup>a</sup>

Entry	Catalyst loading (wt %)	Epoxide yield after (5 h)	Epoxide yield after (10 h)
1	20	50	99
2	10	35	75
3	5	26	56
4	3.5	18	48
5	2.5	12	39
6	2	6	35

<sup>a</sup> Reaction conditions: PVMo/ SiO<sub>2</sub> (0.0475 mmol); olefin (1 mmol); H<sub>2</sub>O<sub>2</sub> (1 mL); CH<sub>3</sub>CN (5 mL), temperature: 78 °C.

**Table 3.** Oxidant selectivity in the oxidation of cyclooctene catalyzed by PVMo/ SiO<sub>2</sub>.<sup>a</sup>

Entry	H <sub>2</sub> O <sub>2</sub> (30%)	Epoxide yield (%)			TONs		
		After 3 h	After 7 h	After 10 h	After 3 h	After 7 h	After 10 h
1	0.5 mL	8	18	27	1.68	3.79	5.68
2	1 mL	24	70	99	5.05	14.74	20.84
3	2 mL	40	85	99	8.42	17.89	20.84
4	3 mL	48	90	99	10.10	18.95	20.84
5	4 mL	54	99	99	11.37	20.84	20.84

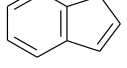
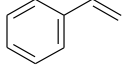
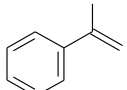
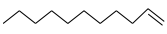
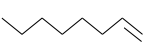
<sup>a</sup>Reaction conditions: PVMo/ SiO<sub>2</sub> (0.0475 mmol); olefin (1 mmol); CH<sub>3</sub>CN (5 mL), temperature: 78 °C.

The epoxidation of cyclooctene was also examined with various amounts of 30% aqueous H<sub>2</sub>O<sub>2</sub> to indicate the oxidant selectivity (Table 3). Therefore, the amount of 1 ml of 30% H<sub>2</sub>O<sub>2</sub> was selected as most favorable amount for oxidant. These studies are beforehand reported by Nomiya [37].

Besides, the results proved that no cyclooctene oxide was detected at room temperature. Thus, all reactions were carried out at 78 °C.

The ability of nanocomposite catalyst (PVMo/ SiO<sub>2</sub>) in the epoxidation of various linear, cyclic and phenyl substituted alkenes as substrate with H<sub>2</sub>O<sub>2</sub> was investigated. The results explain evidently that the conversions, selectivity and TONs are upper for heterogeneous nanocomposite (PVMo/ SiO<sub>2</sub>) in comparison with the homogeneous PVMo (Tables 4).

**Table 4.** Alkene epoxidation with H<sub>2</sub>O<sub>2</sub> catalyzed by PVMo and PVMo/ SiO<sub>2</sub> nanocomposite beneath magnetic stirring (MS) and under ultrasonic irradiation (US).<sup>a</sup>

Entry	Substrate	Conversion (%) <sup>b</sup>			Epoxide yield (%) <sup>b</sup>			TOF(h <sup>-1</sup> )		
		PVMo <sup>c</sup> time(h <sup>-1</sup> )	PVMo/ SiO <sub>2</sub> (MS) <sup>c</sup> / time(h <sup>-1</sup> )	PVMo/ SiO <sub>2</sub> (US) <sup>c</sup> time(min)	PVMo	PVMo/ SiO <sub>2</sub> (MS)	PVMo/ SiO <sub>2</sub> (US)	PVMo	PVMo/ SiO <sub>2</sub> (MS)	PVMo/ SiO <sub>2</sub> (US)
1		100	100	95	95	98	90	1.1	1.1	40
2		85	97	88	70	92	82	0.89	1.02	37.1
3		95	98	92	73	95	85	1.0	1.03	38.7
4		49	85	90	43	78	75	0.51	0.89	37.9
5		29	98	93	27	92	70	0.31	1.03	39.2
6		28	48	65	20	42	60	0.29	0.51	27.4
7		59	68	83	56	65	68	0.62	0.72	34.9
8		31	58	79	28	52	62	0.32	0.61	33.2

<sup>a</sup> Reaction condition: PVMo/ SiO<sub>2</sub> (0.0475 mmol); alkene (1 mmol); H<sub>2</sub>O<sub>2</sub> (1 mL); CH<sub>3</sub>CN (5 mL), temperature: 78 °C.

<sup>b</sup> GC yield.

<sup>c</sup> The reaction time is 20 h for reflux conditions and 30 min for ultrasonic conditions.

The most advantageous conditions which were utilized for alkene epoxidation under ultrasonic irradiation are as what expressed for alkene epoxidation under agitation with magnetic stirring. The reaction mixture was irradiated by ultrasonic waves. The obtained results illustrated that in this catalytic system, the reaction times are shorter and the TONs are higher than mechanical stirring and reflux conditions (Table 4). In the case of  $\alpha$ -pinene, the epoxide yield was enlarged to 60%. The catalytic activity of PVMo/ SiO<sub>2</sub> rose in the epoxidation of linear alkenes such as 1-octene and 1-dodecene, and in the case of norbornene. In contrast with the data obtained under agitation with magnetic stirring, the reaction times are shorter, product yields are higher, and in some case the selectivity enhance.

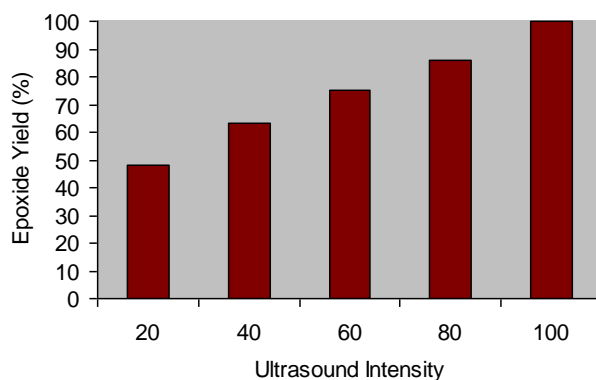


**Figure 8.** The effect of ultrasonic irradiation intensity on the epoxidation of cyclooctene with H<sub>2</sub>O<sub>2</sub> catalyzed by PVMo/ SiO<sub>2</sub>

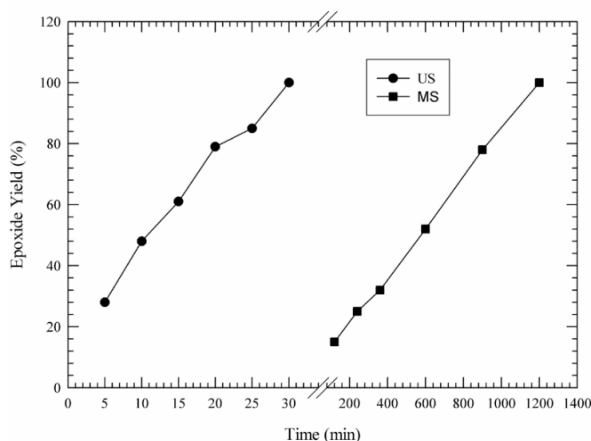
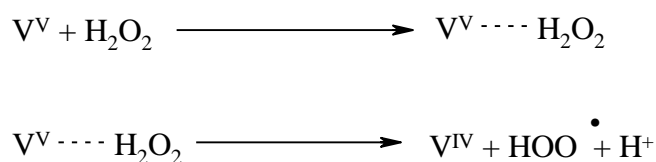


**Figure 9.** Relationship of Ultrasonic irradiation and magnetic agitation in the epoxidation of cyclooctene with H<sub>2</sub>O<sub>2</sub> catalyzed by PVMo/ SiO<sub>2</sub>

The effect of irradiation intensity on the epoxidation of cyclooctene was also investigated; in which the higher epoxide yield was observed at 100% intensity (Fig. 8).

Fig. 9 shows a comparison between systems under ultrasonic irradiation and under agitation with magnetic stirring, which shows the effect of ultrasonic irradiation on the catalytic activity.

As exposed formerly, peroxy radical are generated within the pores at the PVMo sites (Scheme 2). The following oxidation of the hydrocarbon can occur both inside the pores and in the bulk liquid solution [38, 39]. Ultrasonic irradiation encourages the generation of radicals in the reaction media and this can go faster the reaction. Conversely, the collapse of the created bubbles results in production of high temperatures. As the reaction under mechanical stirring requires the temperature about 80 °C, Consequently, the reaction can be also increase speed under ultrasonic irradiation.



**Scheme 2.**

### 3.3. Catalyst reuse and stability

**Table 5.** Epoxidation of cyclooctene with H<sub>2</sub>O<sub>2</sub> (30%) catalyzed by PVMo/ SiO<sub>2</sub> recycled under reflux conditions and under ultrasonic irradiation.<sup>a</sup>

Entry	Reflux conditions				Ultrasonic irradiation			
	Time (h)	Conversion (%)	Epoxide yield (%)	Catalyst leached (%)	Time (min)	Conversion (%)	Epoxide yield (%)	Catalyst leached (%)
1	10	100	98	3	40	98	> 98	2
2	10	85	83	1	40	90	87	1
3	10	80	78	1	40	85	83	1
4	10	75	73	1	40	80	77	1

<sup>a</sup> Reaction condition: PVMo/ SiO<sub>2</sub> (0.0475 mmol); olefin (1 mmol); H<sub>2</sub>O<sub>2</sub> (1 mL); CH<sub>3</sub>CN (5 mL).

The constancy of the nanocomposite PVMo/ SiO<sub>2</sub> was monitored using multiple in order epoxidation reactions both under agitation with magnetic stirring and ultrasonic irradiation. For each of the repeated reactions the catalyst was recovered by simple filtration, washed thoroughly with water, methanol, acetonitrile and 1, 2-dichloroethane, consecutively, and dried before being used.

As exposed in Table 5, the catalyst was successively recovered four times. Although, the solid catalyst has been arranged by non-covalent fixing of the polyoxovanadate anion on chemically modified hydrophobic mesoporous silica [40- 45]. It is expectable that the catalyst leached from silica.

The amount the catalyst, which was leached each run was determined by inductively coupled plasma (ICP) Analysis. The consequences are exposed in Table 5. The nature of recovered catalyst has been followed by IR. The results indicated that the catalyst after recovering several times, demonstrated no significant alter in its IR spectrum.

In table 6. The activity of the supported catalyst with other reported catalysts for the epoxidation of cyclooctene with H<sub>2</sub>O<sub>2</sub> (30%) catalyzed and other reported methods under magnetic stirring (MS) and under ultrasonic irradiation (US) were comprised. The conversion amounts in this method have been the best.

**Table 6.** Comparison of reaction data for the present system in epoxidation of cyclooctene and other reported methods under magnetic stirring (MS) and under ultrasonic irradiation (US) in almost conditions .<sup>a</sup>

Entry	Substrate	Conversion (%) <sup>b</sup>			Epoxide yield (%) <sup>b</sup>			Ref
		PVMO <sup>c</sup> time(h <sup>-1</sup> )	(MS) <sup>c</sup> / time(h <sup>-1</sup> )	(US) <sup>c</sup> time(min)	PVMO	(MS)	(US)	
1	PVMO/ SiO <sub>2</sub>	100	100	95	95	98	90	This paper
2	PVMO/ CNTs	78	80	95	96	100	100	[19]
3	PVMO /MMT	55	58	71	96	65	77	[17,23]
4	PVMO/ PANI	52	62	90	90	89	98	[20]
5	PVMO/ ZrO <sub>2</sub>	55	70	93	95	80	97	[21]
6	PVMO/ TiO <sub>2</sub>	78	85	98	96	100	100	[22]

<sup>a</sup> Reaction condition: PVMO/ SiO<sub>2</sub> (0.0475 mmol); alkene (1 mmol); H<sub>2</sub>O<sub>2</sub> (1 mL); CH<sub>3</sub>CN (5 mL)

<sup>b</sup> GC yield.

<sup>c</sup> The reaction time is 20 h for reflux conditions and 30 min for ultrasonic conditions.

#### 4. CONCLUSIONS

We productively produced the PVMO/ SiO<sub>2</sub> nanocomposite by straightforward impregnation technique. The as-prepared nanocomposite demonstrated higher catalytic activity for epoxidation of

alkenes than parent heteropolymolybdate (PVMo). The use of ultrasonic irradiation enhanced the conversion and decreased the reaction times. The consequences explained that excellent catalytic activity of the heteropolymolybdate; particularly under ultrasonic irradiation make them valuable catalysts for extra applications in the region of catalysis. Moreover, the H<sub>2</sub>O<sub>2</sub> is a green and eco-friendly oxidant in these arrangements. The performed search on the electrochemical presentation of the dissolved heteropolymolybdate distinguishes it as an outstanding electroactive for the H<sub>2</sub>O<sub>2</sub> reduction. The polyoxoanion, immobilized in a mesoporous silica matrix, qualitatively retained its electrochemical behavior displayed in solution, but for both the immobilization matrix the electrocatalytic effectiveness and the sensitivity toward H<sub>2</sub>O<sub>2</sub> reduction were superior.

#### ACKNOWLEDGEMENTS

The support of this work by Catalysis Division of University of Payame Noor University (PNU) and Chemistry department of Isfahan University (CECUI) is acknowledged.

#### References

1. J. Zhang, L. Xu, Y. Cui, W. Cao, Z. Li, *Mat. Chem. Phy* 90 (2005) 47-52.
2. H. Jong Kim, Y. Gun Shul, H. Han, *Appl. Catal. A: Gen* 299 (2006) 46-51.
3. S. Damyanova, L. Dimitrov, R. Mariscal, J.L.G. Fierro, L. Petrov, I. Sobrados, *Appl. Catal. A: Gen* 256 (2003) 183-197.
4. L. Zhang, Q. Jin, L. Shan, Y. Liu, X. Wang, J. Huang, *Appl. Clay Sci.* 47 (2010) 229-234.
5. I. V. Kozhevnikov, *J. Mol. Catal. A: Chem.* 262 (2007) 86-92.
6. Y. Tang, J. Zhang, *Trans. Met. Chem.*, 31 (2006) 299-305.
7. Y.L. Shi, W. Qiu, J. Zhang, *J. Phys. Chem. Solids.* 67 (2006) 2409-2418.
8. T. Okuhara, N. Mizuno, M. Misono, *Adv. Cata.* 41 (1996) 113-252.
9. M. Misono, I. Ono, G. Koyano, A. Aoshima, *Pure. Appl. Chem.* 72 (2000) 1305-1311.
10. K. Nowinska, R. Fiedorow, J. Adamiec, *J. Chem. Soc., Faraday Trans.* 87 (1991) 749-753.
11. W.C. Cheng, N. P. Luthra, *J. Catal.* 109 (1988) 163-169.
12. K. M. Rao, R. Gobetto, A. Iannibello, A. Zecchina, *J. Catal.* 119 (1989) 512-516.
13. H.J. Kim, Y.G. Shul, H. Han, *Appl. Catal. A: Gen* 299 (2006) 46-51.
14. L. R. Pizzio, C. V. Cáceres, M. N. Blanco, *Appl. Catal., A Gen.* 167 (1998) 283-294.
15. D. Kumar, C. C. Landry, *Micropor. Mesopor. Mat.* 98 (2007) 309-316.
16. B.M. Devassy, F. Lefebvre, W. Böhringer, J. Fletcher, S.B. Halligudi, *J. Mol. Catal A: Chem* 236 (2005) 162-167.
17. H. Salavati, S. Tangestaninejad, M. Moghadam, V. Mirkhani, I. Mohammadpoor-Baltork, *Ultrason. Sonochem* 17 (2010) 145-152.
18. H. Salavati, N. Rasouli, *Mater. Res. Bull.* 46 (2011) 1853-1859.
19. H. Salavati, S. Tangestaninejad, M. Moghadam, V. Mirkhani, I. Mohammadpoor-Baltork, *Ultrason. Sonochem* 17 (2010) 453-459.
20. S. Tangestaninejad, M. Moghadam, V. Mirkhani, I. Mohammadpoor-Baltork, E. Shams, H. Salavati, *Catal. Commu* 9 (2008) 1001-1009.
21. H. Salavati, S. Tangestaninejad, M. Moghadam, V. Mirkhani, I. Mohammadpoor-Baltork, *Comptes. Rendus. Chimie.* 14 (2011) 588-596.
22. H. Salavati, N. Rasouli, *Appl. sur. sci.* 257 (2011) 4532-4538.
23. O.A. Kholdeeva, N.V. Maksimchuk, G.M. Maksimov, *Catal. Today* 157 (2010) 107-113.

24. L R. Pizzio, C. V. Cáceres, M. N. Blanco, *J. Coll. Interf. Sci.* 190 (1997) 318-326.
25. T. Baba, Y. Ono, *Appl Catal* 22 (1986) 321-324.
26. S. Gaspar, L. Muresan, A. Patrut, I. C. Popescu, *Anal. Chim. Acta*, 385 (1999) 111-117.
27. A. Teimouri, A. Najafi Chermahini, *J. Mol. Catal A: Chem.* 346 (2011) 39-45.
28. A. Teimouri, A. Najafi Chermahini, H. Salavati, L. Ghorbanian, *J. Mol. Catal A: Chem.* 373 (2013) 38-45.
29. Y. Izumi, K. Hisano, T. Hida, *Appl. Catal. A: Gen* 181 (1999) 277-282.
30. J. Toufaily, M. Soulard, J.-L. Guth, J. Patarin, L. Delmote, T. Hamieh, M. Kodeih, D. Naoufal, H. Hamad, *Collo. Surf. A: Physicochem. Eng. Aspects* 316 (2008) 285-291.
31. L. Pettersson, I. Andersson, A. Selling, G. H. Grate, *Inorg. Chem.* 33 (1994) 982-993.
32. P. Stati, S. Freni, S. Hocevar, *J. Power Sources* 79 (1999) 250-255.
33. M. A. Hamon, H. Hu, P. Bhowmik, S. Niyogi, B. Zhao, M. E. Itkis, R. C. Haddon, *Chem. Phys. Lett.* 347 (2001) 8-12.
34. N. K. Kala Raj, A. V. Ramaswamy, P. Manikandan, *J. Mol. Catal A: Chem.* 227 (2005) 37-45.
35. K. S. W. Sing; D. H. Everett, R. A. W. Haul, L. Moscou; R. A. Pierotti; J. Rouquerol; T. Siemieniewska, *Pure & Appl. Chem* 57(4) (1985) 603-619.
36. D. Chandra, B.K. Jena, C.R. Raj, A. Bhaumik, *Chemistry of Materials* 19 (2007) 6290–6296.
37. K. Nomiya, K. Yagishita, Y. Nemoto, T. A. Kamataki, *J. Mol. Catal.* 126 (1997) 43.
38. B. R. Limonges, R. J. Stains, J. A. Turner, A. M. Herring, *Electrochim. Acta* 50 (2005) 1169-1179.
39. Y.T. Chang, K.C. Lin, S.M. Chen, *Electrochim. Acta* 51 (2005) 450-461.
40. S. Inagaki, Y. Fukushima, K. Kuroda, *Journal of the Chemical Society, Chem. Commun* (1993) 680–681.
41. S. Gaspar, L. Muresan, A. Patrut, I. C. Popescu, *Anal. Chim. Acta* 385 (1999) 111-117.
42. H. Salavati, H. Saedi, *Int. J. Electrochem. Sci.*, 10 (2015) 4208 – 4222.
43. K. Nomiya, S. Matsuoka, T. Hesegawa, Y. J. Nemoto. *J. Mol. Catal A: Chem* 156 (2000) 143-152.
44. A. M. Khenkin, R. Neumann, A. B. Sorokin, A. Tuel, *Catal. Lett.* 63 (1999) 189-192.
45. C. Shi, R. Wang, G. Zhu, S. Qiu, J. Long, *Eur. J. Inorg. Chem* (2005) 4801-4807.